Available online at www.sciencedirect.com
SCIENCE DIRECT®
International Journal of Engineering Science 42 (2004) 243–256
International Journal of Engineering Science
www.elsevier.com/locate/ijengsci

Effect of thermophysical quantities on the natural convection flow of gases over a vertical cone

H.S. Takhar [a,*], A.J. Chamkha [b], G. Nath [c]

[a] Department of Engineering, Manchester Metropolitan University, Oxford Road, Manchester M1 5 GD, UK
[b] Department of Mechanical Engineering, Kuwait University, Safat 13060, Kuwait
[c] Department of Mathematics, Indian Institute of Science, Bangalore 560012, India

Received 28 May 2003; accepted 30 July 2003

(Communicated by E.S. ŞUHUBİ)

Abstract

The laminar steady nonsimilar natural convection flow of a gases over an isothermal vertical cone has been investigated where the thermal conductivity, dynamic viscosity and specific heat at constant pressure are assumed to have a power-law variation with absolute temperature. The density is taken as inversely proportional to the absolute temperature, whereas the Prandtl number is assumed to be constant. The nonlinear coupled parabolic partial differential equations have been solved numerically by using an implicit finite-difference scheme. The variable gas properties significantly affects the heat transfer and skin friction. The heat transfer and skin friction decrease with increasing wall temperature ratio and the streamwise distance. The heat transfer increases with suction, but decreases with injection.

Keywords: Natural convection; Variable physical properties

1. Introduction

Natural convection phenomena arise in nature as well as in industries when a heated surface is brought into contact with a mass of fluid. Consequently, the temperature difference causes density variations leading to buoyancy forces. This mode of heat transfer is encountered in

* Corresponding author. Tel.: +44-161-247-3668; fax: +44-161-247-1633.
E-mail address: h.s.takhar@mmu.ac.uk (H.S. Takhar).

0020-7225/$ - see front matter © 2003 Elsevier Ltd. All rights reserved.
doi:10.1016/j.ijengsci.2003.07.005

atmospheric and oceanic circulations, in the handling of spent nuclear reactor fuel assembles, in the design of solar energy collectors, in the process of frost formation involving low-temperature surfaces etc. Natural convection from a vertical surface with constant fluid properties been extensively studied. Gebhart et al. [1] have presented an overview of natural convection flows. In many problems the fluid properties are not constant. Sparrow and Gregg [2] studied the effects of the ariable fluid properties on the free convection flow over an isothermal vertical flat plate. Brown [3] examined the effect of the coefficient of volumetric expansion on the natural convection heat transfer. Gray and Giogins [4] discussed the validity of the Boussinesq approximation and studied the free convection flows with fluid properties varying linearly with temperature. Miyamoto [5] considered the effect of the variable fluid properties on transient and steady state natural convection flows on an isothermal vertical surface. Clausing and Kempka [6] presented their experimental study of the influence of the variable fluid properties on the natural convection on a vertical plate. Shang and Wang [7] examined the effect of the power-law variations of the thermal conductivity and dynamic viscosity with temperature, on the free convection flow of gases over an isothermal vertical surface and obtained a self-similar solution of the boundary layer equations. Recently, Pantokratoras [8] has studied the effect of the variable fluid properties on the natural convection flow of pure and saline water along a vertical isothermal cylinder.

The present analysis deals with the effect of the thermophysical quantities of gases on the steady laminar natural convection flow over an isothermal vertical cone where the dynamic viscosity $\mu \propto T^{W_1}$, the thermal conductivity $K \propto T^{W_2}$ and the specific heat at a constant pressure $C_p \propto T^{W_3}$. Here T is the absolute temperature and W_1, W_2 and W_3 are positive constants. The gas density ρ is assumed to vary inversely as T and Prandtl number Pr is taken as a constant. The nonlinear coupled parabolic partial differential equations have been solved numerically by using an implicit finite-difference scheme similar to that of Blottner [9]. The results corresponding to the constant fluid properties have been compared with those of Watanabe [10].

2. Analysis

Let us consider a vertical circular cone (Fig. 1) with a semi-vertical angle Ω placed in an otherwise ambient fluid with constant temperature T_∞. The surface of the cone is maintained at a constant temperature T_w. Here we have assumed power-law variations of gas viscosity, thermal conductivity and specific heat with temperature [7]. The density is taken to be inversely proportional to temperature and the Prandtl number is assumed to be constant. It is possible to neglect the effect of the buoyancy induced streamwise pressure gradient if $\Omega \leqslant \Omega_0$ [11]. Under the above assumptions, the conservation equations for the steady laminar boundary layer flow over an isothermal vertical cone can be expressed as,

$$\frac{\partial}{\partial x}(\rho r u) + \frac{\partial}{\partial y}(\rho r v) = 0, \tag{1}$$

$$\rho\left(u\frac{\partial u}{\partial x} + v\frac{\partial u}{\partial y}\right) = \frac{\partial}{\partial y}\left(\mu\frac{\partial u}{\partial y}\right) + g\beta(T - T_\infty)\cos\Omega, \tag{2}$$

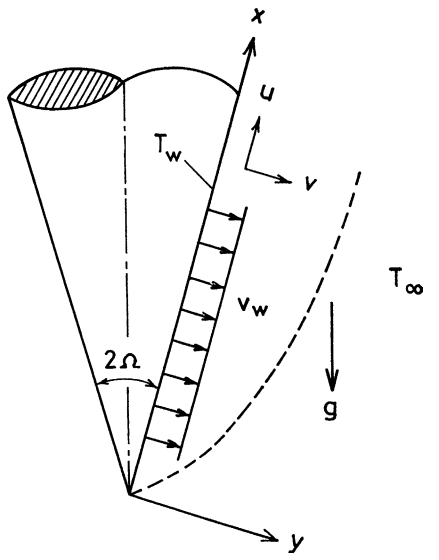

Fig. 1. The coordinate system.

$$\rho C_p\left(u\frac{\partial T}{\partial x}+v\frac{\partial T}{\partial y}\right)=\frac{\partial}{\partial y}\left(K\frac{\partial T}{\partial y}\right). \tag{3}$$

The boundary conditions on the wall are the no-slip conditions and far away from the surface these are given by ambient conditions. These conditions are expressed as,

$$\begin{aligned} &u(x,0)=0, \quad v(x,0)=v_w, \quad T(x,0)=T_w,\\ &u(x,\infty)=0, \quad T(x,\infty)+T_\infty,\\ &u(0,y)=0, \quad T(0,y)+T_\infty, \quad y>0. \end{aligned} \tag{4}$$

Here x is the distance along the surface of the cone from the apex; $x=0$ is the leading edge y; measures the distance normally outward; u and v are the velocity components along the x and y directions, respectively; ρ is the density; K and μ are the thermal conductivity and dynamic viscosity, respectively; C_p is the specific heat at a constant pressure; T is the temperature; g is the acceleration due to gravity; $r(=x\sin\mu)$ is the local cone radius; β is the volumetric coefficient of thermal expansion; and the subscripts w and ∞ denote conditions at the wall and in the ambient fluid, respectively.

It is convenient to transform the governing equations (1)–(3) to dimensionless form by applying the following transformations

$$\begin{aligned} &X=x/L, \quad Y=y/L, \quad R=r/L, \quad U=uL/v_\infty \quad V=vL/v_\infty,\\ &\theta=(T-T_\infty)/(T_w-T_\infty), \quad R=X\sin\Omega, \quad Gr_L=g\beta(T_w-T_\infty)L^3/v_\infty^2,\\ &Pr=\mu_\infty C_{p_\infty}/K_\infty. \end{aligned} \tag{5}$$

Consequently, Eqs. (1)–(3) reduce to

$$\frac{\partial}{\partial X}(\rho UR) + \frac{\partial}{\partial Y}(\rho UR) = 0, \tag{6}$$

$$U\frac{\partial U}{\partial X} + V\frac{\partial U}{\partial Y} = \frac{\rho_\infty}{\rho}\frac{\partial}{\partial Y}\left(\frac{\mu}{\mu_\infty}\frac{\partial U}{\partial Y}\right) + Gr_L\theta\cos\Omega, \tag{7}$$

$$U\frac{\partial \theta}{\partial X} + V\frac{\partial \theta}{\partial Y} = \frac{\rho_\infty}{\rho}\frac{C_{p_\infty}}{C_p}Pr^{-1}\frac{\partial}{\partial Y}\left(\frac{K}{K_\infty}\frac{\partial \theta}{\partial Y}\right). \tag{8}$$

The boundary conditions (4) can be re-written as

$$\begin{aligned} &U(X,0) = 0, \quad V(X,0) = V_{\mathrm{w}} = L/v_\infty, \\ &U(X,\infty) = 0, \quad \theta(X,\infty) = 0. \end{aligned} \tag{9}$$

Here X and Y are the dimensionless distances along and perpendicular to the surface; U and V are the dimensionless velocity components along X and Y directions; θ is the dimensionless temperature; L is the characteristic length; R is the dimensionless local radius of the cone; Pr is the Prandtl number; and Gr_L is the Grashof number.

In order to reduce the number of equations from three to two, we introduce the stream function Ψ and use the transformations given by

$$\begin{aligned} &\rho UR = \rho_\infty \partial\psi/\partial Y, \quad -\rho VR = \rho_\infty \partial\psi/\partial X, \quad \xi = X, \\ &\eta = (Gr_L/\xi)^{1/4}\int_0^Y (\rho/\rho_\infty)\,\mathrm{d}Y, \quad \psi(X,Y) = RGr_L^{1/4}\xi^{3/4}f(\xi,\eta), \\ &U = U^* f'(\xi,\eta), \quad U^* = (Gr_L\xi)^{1/2}, \quad A = (T_{\mathrm{w}} - T_\infty)/T_\infty, \\ &V = -(\rho_\infty/\rho)Gr_L^{1/4}\xi^{-1/4}[(7/4)f + \xi\partial f/\partial\xi], \\ &f_{\mathrm{w}} = B\xi^{1/4}, \quad \rho_\infty/\rho = T/T_\infty, \quad \mu/\mu_\infty = (T/T_\infty)^{W_1}, \\ &K/K_\infty = (T/T_\infty)^{W_2}, \quad C_p/C_{p_\infty} = (T/T_\infty)^{W_3}, \quad W_3 = W_2 - W_1, \\ &N = \rho\mu/\rho_\infty\mu_\infty = (T/T_\infty)^{W_1-1}, \quad N_1 = \rho K/\rho_\infty K_\infty (T/T_\infty)^{W_2-1}, \\ &T/T_\infty = 1 + A\theta, \quad B = -2^{-1}Gr_L^{-1/4}(\rho_{\mathrm{w}}/\rho_\infty)V_w. \end{aligned} \tag{10}$$

In Eq. (6)–(8), we find that Eq. (6) is identically satisfied and Eqs. (7) and (8) reduce to

$$(Nf'')' + (7/4)ff'' - 2^{-1}f'^2 + \theta\cos\Omega = \xi(f'\partial f'/\partial\xi - f''\partial f/\partial\xi), \tag{11}$$

$$(N_1\theta')' + (7/4)Pr(C_p/C_{p_\infty})f\theta' = Pr(C_p/C_{p_\infty})\xi(f'\partial\theta/\partial\xi - \theta'\partial f/\partial\xi). \tag{12}$$

Table 1
The value of the parameters, Pr, W_1, W_2, and W_3

	Ar	H_2	Air	N_2	CO	O_2	Water vapour
Pr	0.622	0.68	0.70	0.71	0.72	0.733	1.0
W_1	0.72	0.68	0.68	0.67	0.71	0.694	1.04
W_2	0.73	0.80	0.81	0.76	0.83	0.860	1.185
W_3	0.01	0.12	0.13	0.09	0.12	0.166	0.145

The boundary conditions (9) can be expressed as

$$\begin{aligned} &f(\xi,0) = f_w = B\xi^{1/4}, \quad f'(\xi,0) = 0, \quad \theta(\xi,0) - 1, \\ &f'(\xi,\infty) = \theta(\xi,\infty) = 0. \end{aligned} \tag{13}$$

Here ξ and η are the transformed coordinates; Ψ is the dimensionless stream function; f is the transformed stream function; W_1 W_2 and W_3 are positive constants; N and N_1 are functions of θ; A is the temperature ratio defined in Eq. (1) and $A > 0$ for $T_w > T_\infty$ and $A < 0$ for $T_w < T_\infty$; f_w is the mass transfer function; B is a constant if the normal velocity at the wall V_w is constant and $B \geqslant 0$ according to whether there is suction or injection; U^* is the hypothetical or equivalent velocity at the edge of the boundary layer.

Following Shang and Wang [7] we have taken power-law variations of the thermophysical properties of the gases with temperature as given in Eq. (1). These are found to be in good agreement with the experimental values [7]. The values of W_1, W_2, W_3 and Pr for various gases are given in Table 1. When the gases have constant properties, $W_1 = W_2 = 1$, $W_3 = 0$. Hence $N = N_1 = C_p/C_{p_\infty} = 1$.

The local skin friction and heat transfer coefficients can be expressed as

$$\begin{aligned} &Cf_x = \mu_w(\partial u/\partial y)_{y=0}/\rho_\infty(U^* v_\infty/L)^2 = (1+A)^{W_1-1} Gr_x^{-1/4} f''(\xi,0), \\ &Nu_x = -K_w(\partial T/\partial y)_{y=0} x/K_\infty(T_w - T_\infty) = -(1+A)^{W_2-1} Gr_x^{1/4}\theta'(\xi,0), \end{aligned} \tag{14}$$

where Cf_x is the local skin friction coefficient, Nu_x is the local Nusselt number, v is the kinematic viscosity and $Gr_x (= g\beta(T_w - T_\infty)x^3/v_\infty^2)$ is the Grashof number defined with respect to x.

3. Methods of solution

The partial differential equations (11) and (12) under the conditions (13) have been solved numerically using an implicit finite-difference scheme similar to that of Blottner [9]. All the first order derivatives with respect to ξ have been replaced by two-point backward difference formulae

$$\partial R/\partial\xi = (R_{i,j} - R_{i-1,j})/\Delta\xi, \tag{15}$$

where R is the dependent variable f' or θ and i and j are the node locations along ξ and η directions, respectively. The third-order partial differential equation (11) is converted to a

second-order by substitutions $f' = F$. The second-order equations are discretized by using three-point central difference formulae while the first-order derivatives with respect to η are discretized by using the trapezoidal rule. At each line of constant ξ, a system of algebraic equations is solved iteratively by using the Thomas algorithm (see Blottner [9]). The same process is repeated for the next ξ value and the equations are solved line by line until the desired ξ value is reached. A convergence criterion based on the relative difference between the current and previous iterations has been used. When this difference becomes 10^{-5}, the solution is assumed to have converged and the iterative process is terminated.

We have carried out the sensitivity analysis of the step size $\Delta\xi$ and $\Delta\eta$ and the edge of the boundary layer η_∞ on the solution. Finally we have taken $\Delta\eta = 0.025$, $\Delta\xi = 0.05$, $\eta_\infty = 12$.

4. Results and discussion

Eqs. (11) and (12) under the conditions (13) have been solved numerically by using an implicit finite difference scheme described earlier. In order to assess the accuracy of our method, we have compared our skin friction and heat transfer results for $\xi = 0$, $\Omega = \pi/6$, $Pr = 0.73$, $W_1 = W_2 = 1$, $W_3 = 0$ (self-similar flow with constant fluid properties) with those Watanabe [10]. The results are found to be in good agreement and the comparison is presented in Table 2.

The effect of wall temperature ratio A ($A > 0$ for $T_w > T_\infty$ and $A < 0$ for $T_w < T$) on the velocity and temperature profiles, $f'(\xi,\eta)$ and $\theta(\xi,\eta)$, for Ar, N_2 and water vapour $\xi = 1$, $\Omega = \pi/6$, $B = -0.5$ is in shown in Figs. 2 and 3. The maximum velocity for $A > 0$ ($T_w > T_\infty$) is more than that for $A < 0$ ($T_w < T_\infty$), because for gases the viscosity increases with temperature. Consequently the boundary layer thickness increases. Also the momentum and thermal boundary layers for water vapour or N_2 is less that that of Ar, because the Prandtl number Pr for water vapour ($Pr = 1.0$) or N_2 ($Pr = 0.7$) is more than that of Ar ($Pr = 0.622$). The increase in Pr results in thinner boundary layers.

Figs. 4 and 5 present the effect of semi-vertical angle of the cone Ω on the velocity and temperature profiles, $f'(\xi,\eta)$ and $\theta(\xi,\eta)$, for Ar and water vapour when $A = 1$, $B = -0.5$, $\xi = 1$. Both

Table 2
Comparison of skin friction and heat transfer parameters, $f''(0)$ and $\theta'(0)$, for $\xi = 0$, $Pr = 0.73$, $\Omega = \pi/6$, $W_1 = W_2 = 1$, $W_3 = 0$

B	Present results		Watanabe [10]	
	$f''(0)$	$-\theta'(0)$	$f''(0)$	$-\theta'(0)$
0.7	0.41721	3.99125	0.41776	3.99260
0.5	0.59018	2.81342	0.59075	2.81470
0.3	0.81003	1.78663	0.81037	1.78792
0.1	0.87496	0.98408	0.87550	0.98535
0	0.84017	0.67746	0.84043	0.67894
−0.1	0.77053	0.43779	0.77029	0.43799
−0.3	0.58664	0.13978	0.58642	0.13997
−0.5	0.42012	0.02756	0.42002	0.02743

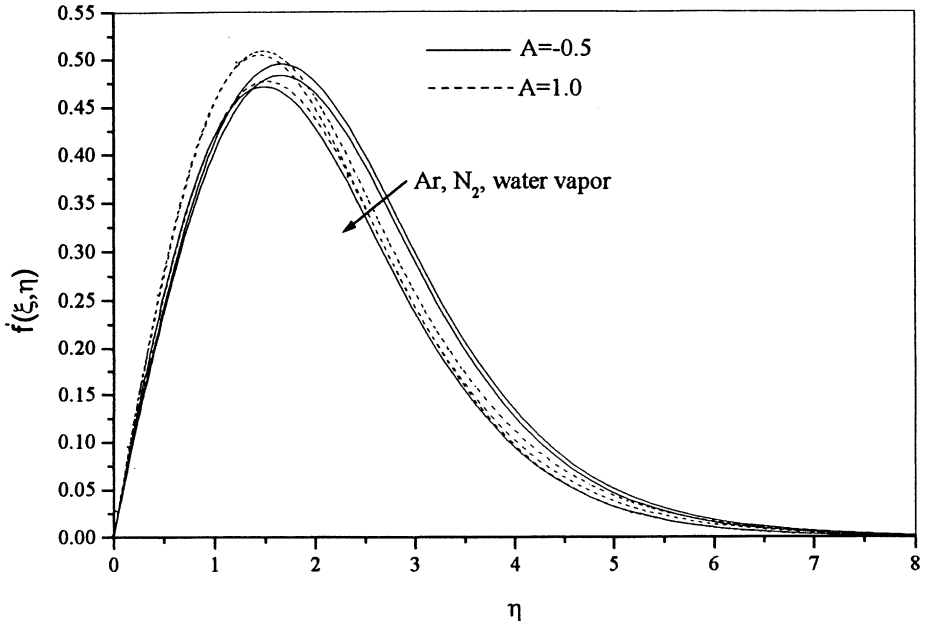

Fig. 2. Effect of the wall temperature ratio, A, on the velocity profiles, $f'(\xi,\eta)$, for Ar, N_2 and water vapour.

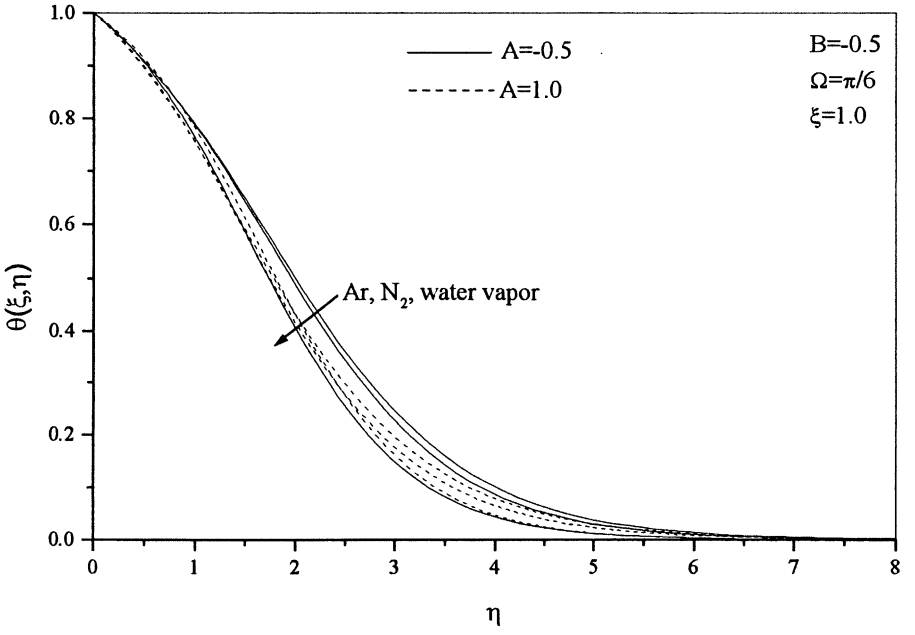

Fig. 3. Effect of the wall temperature ratio, A, on the temperature profiles, $\theta(\xi,\eta)$, for Ar, N_2 and water vapour.

the momentum and thermal boundary layer thicknesses increase with Ω. The increase in Ω implies that the magnitude of the buoyancy force is reduced (see Eq. (11)). Hence the deriving mechanism of the flow becomes weak which in turn causes thicker boundary layers.

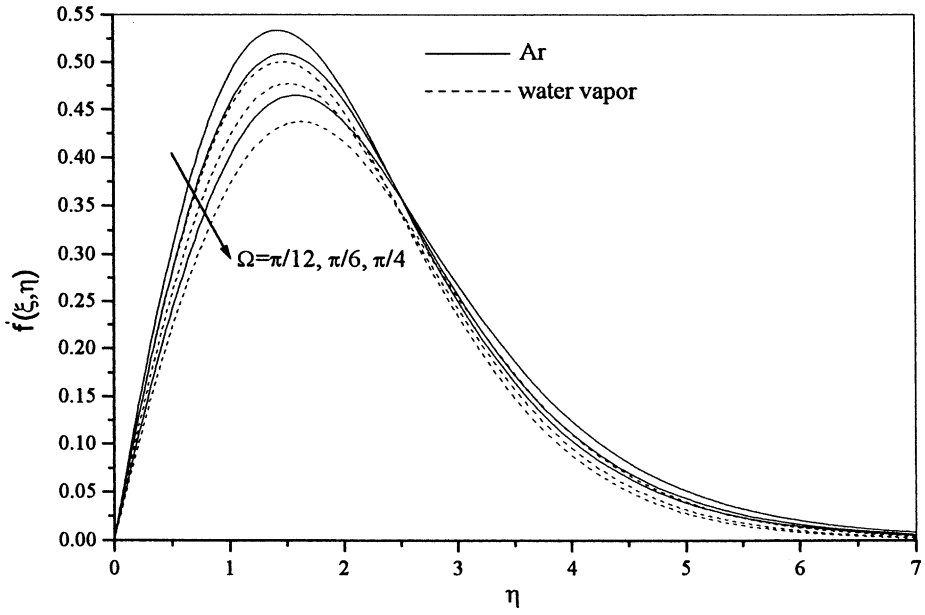

Fig. 4. Effect of the semi-vertical angle of the cone, Ω, on the velocity profiles $f'(\xi,\eta)$, for Ar and water vapour.

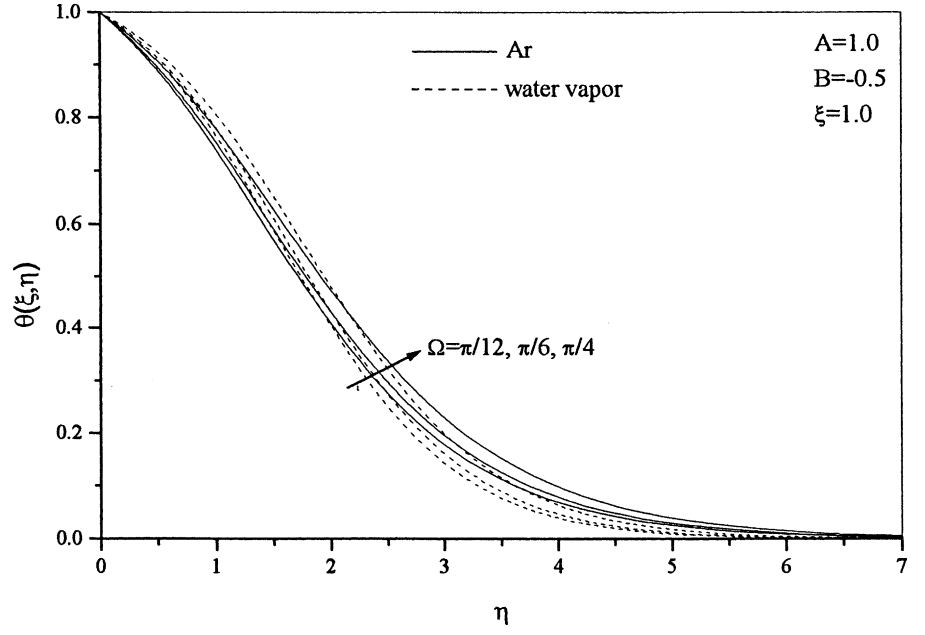

Fig. 5. Effect of the semi-vertical angle of the cone, Ω, on the temperature profiles, $\theta(\xi,\eta)$, for Ar and water vapour.

Figs. 6–13 present the variation of the local skin friction coefficient, $Gr_x^{1/4}C_{fx}$, and the local Nusselt number, $Gr_x^{-1/4}Nu_x$, with the streamwise distance ξ $(0 \leqslant \xi \leqslant 2)$ for Ar, air, O_2 and water

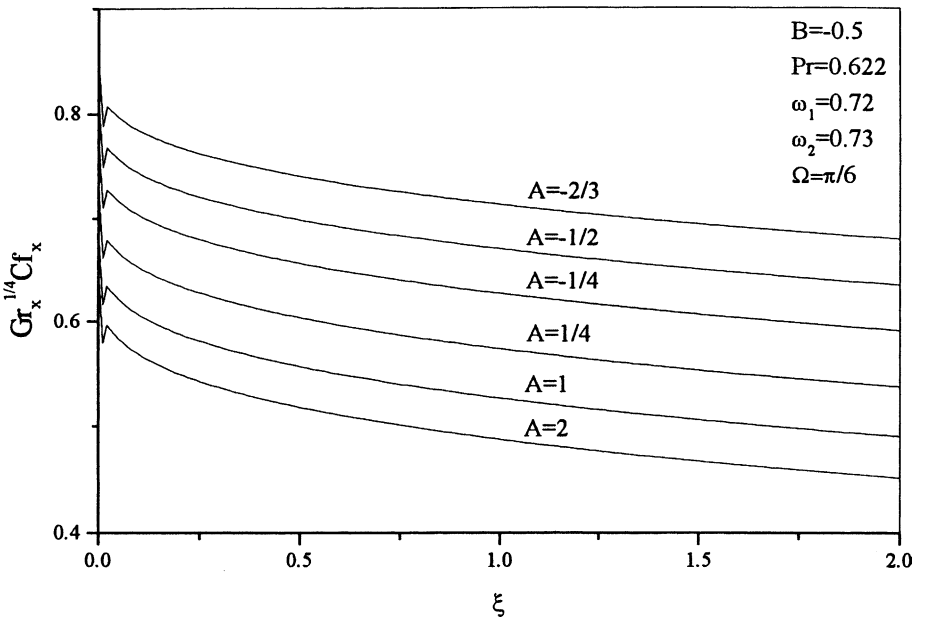

Fig. 6. Effect of the wall temperature ratio, A, on the variations of the local skin friction coefficient, $Gr_x^{1/4}Cf_x$, with the streamwise distance ξ for Ar.

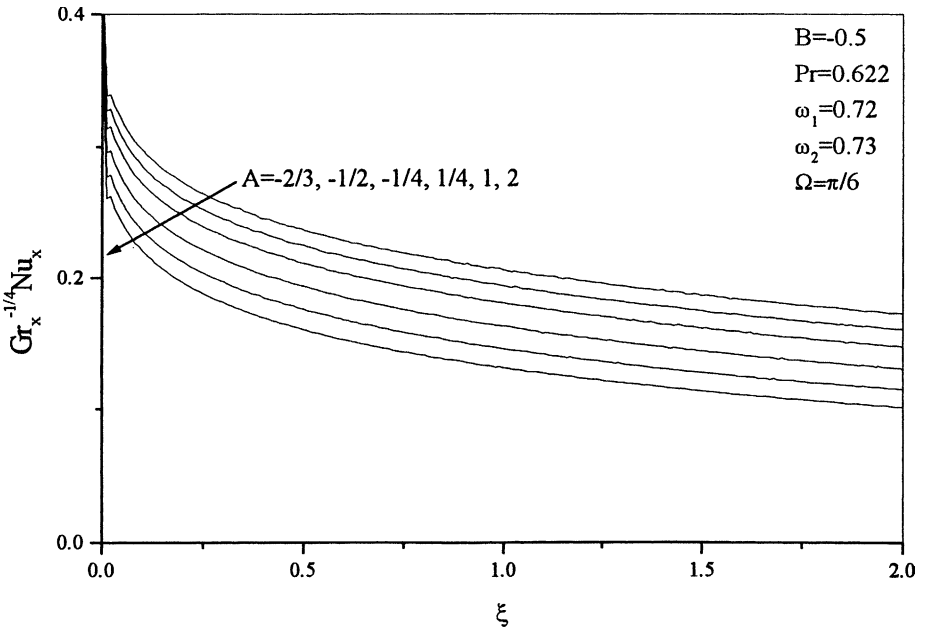

Fig. 7. Effect of the wall temperature ratio, A, on the variations of the local Nusselt number, $Gr_x^{-1/4}Nu_x$, with the streamwise distance ξ for Ar.

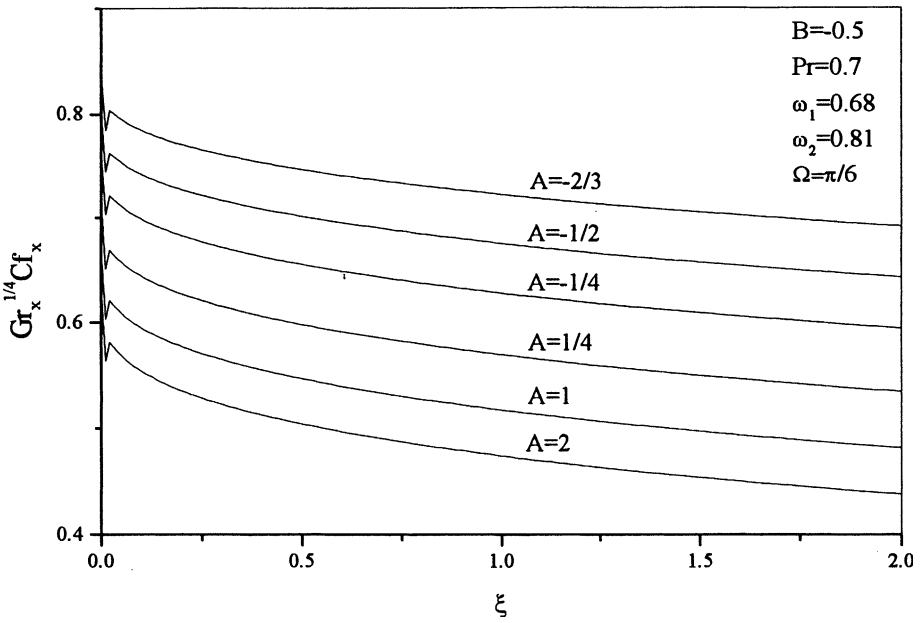

Fig. 8. Effect of the wall temperature ratio, A, on the variations of the local skin friction coefficient, $Gr_x^{1/4}Cf_x$, with the streamwise distance ξ for air.

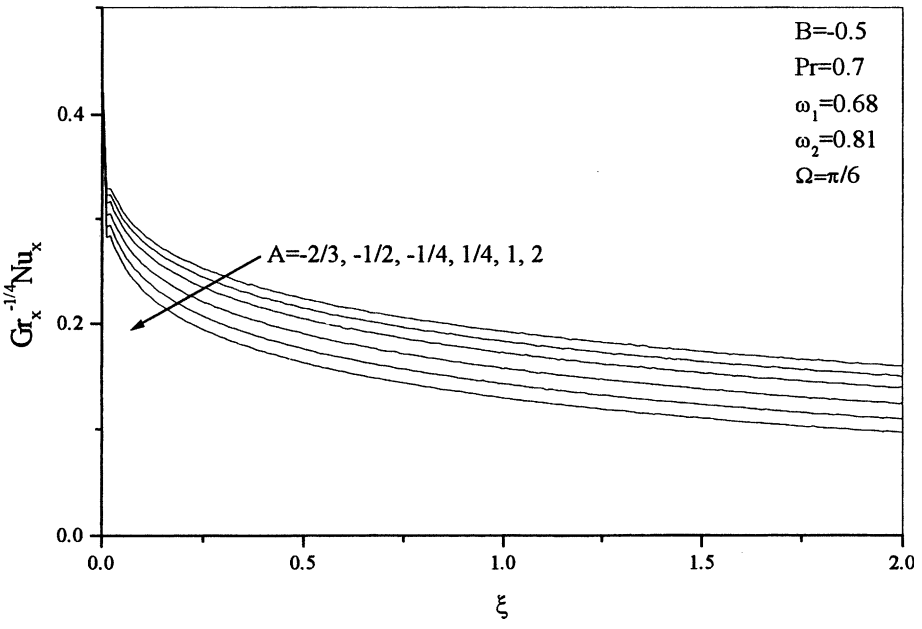

Fig. 9. Effect of the wall temperature ratio, A, on the variations of the local Nusselt number, $Gr_x^{-1/4}Nu_x$, with the streamwise distance ξ for air.

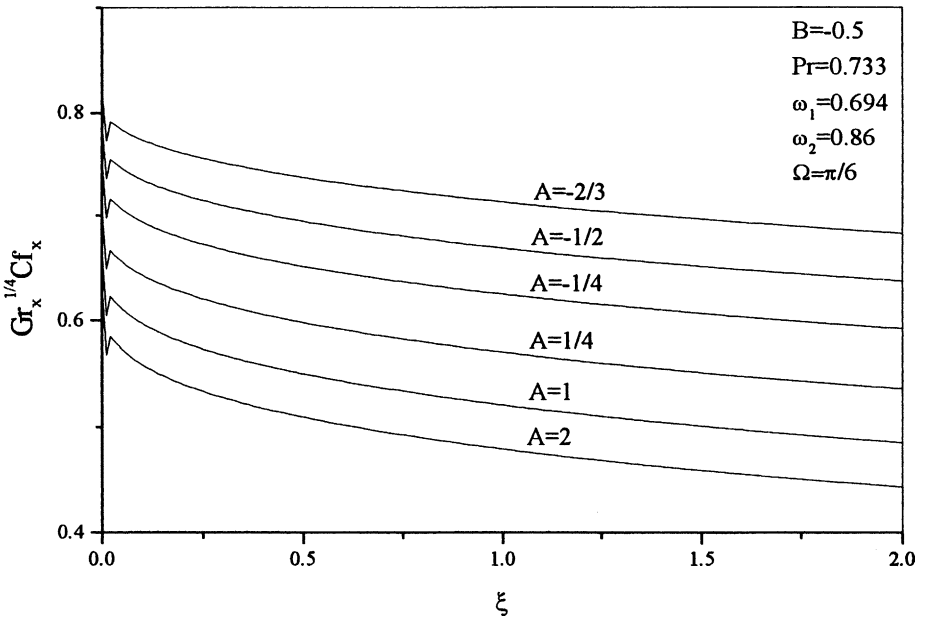

Fig. 10. Effect of the wall temperature ratio, A, on the variations of the local skin friction coefficient, $Gr_x^{1/4}Cf_x$, with the streamwise distance ξ for a O_2.

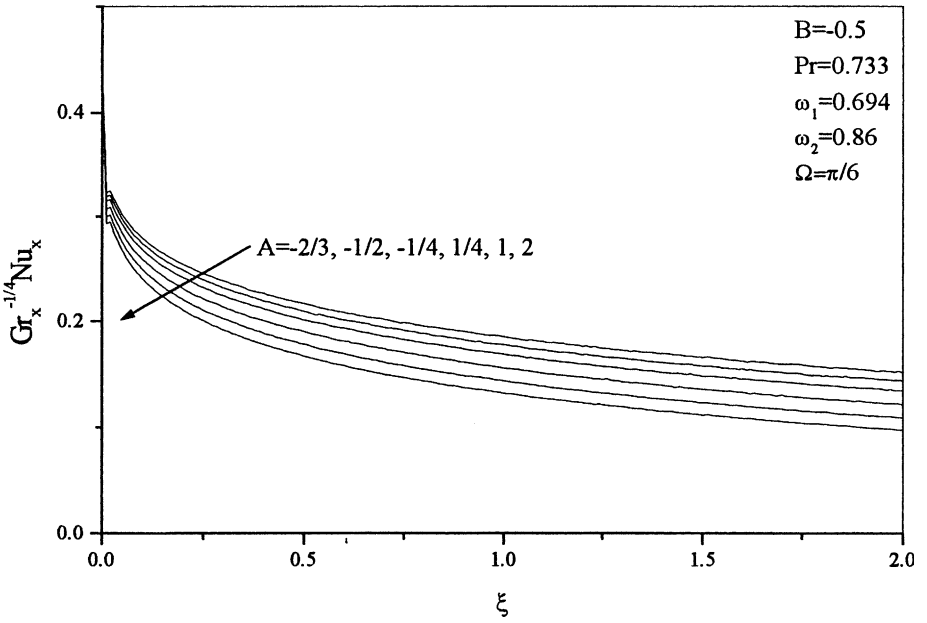

Fig. 11. Effect of the wall temperature ratio, A, on the variations of the local Nusselt number, $Gr_x^{-1/4}Nu_x$, with the streamwise distance ξ for O_2.

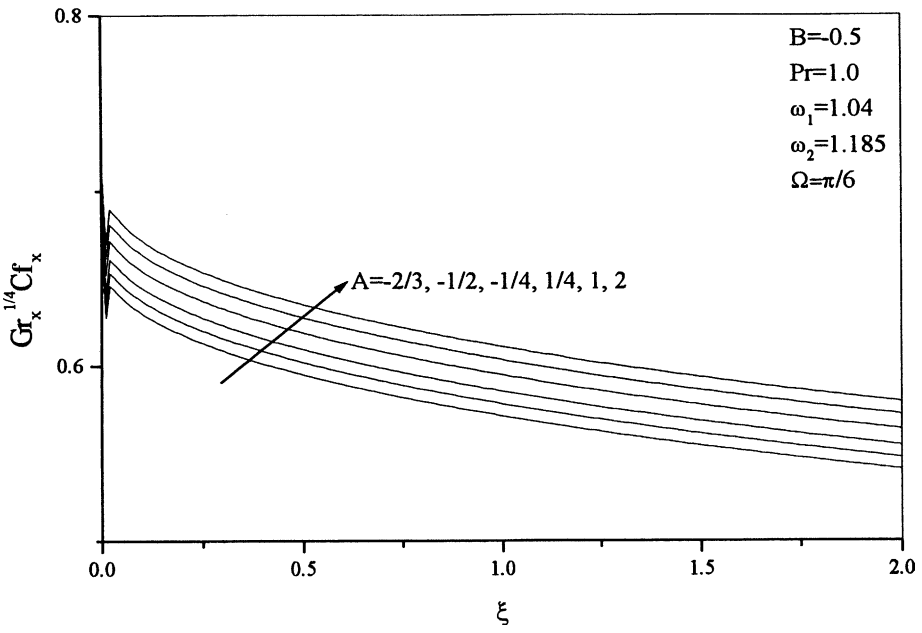

Fig. 12. Effect of the wall temperature ratio, A, on the variations of the local skin friction coefficient, $Gr_x^{1/4}Cf_x$, with the streamwise distance ξ for water vapour.

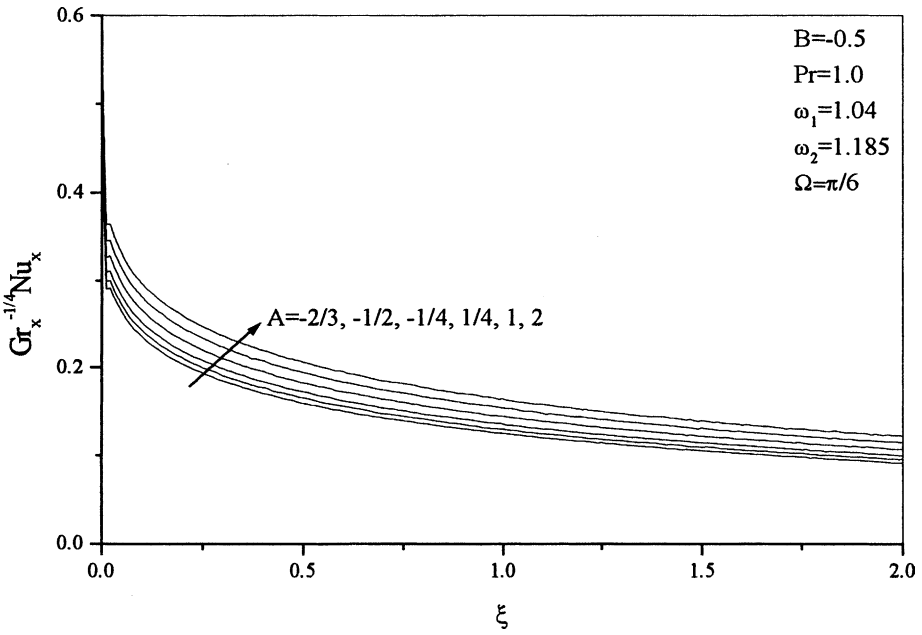

Fig. 13. Effect of the wall temperature ratio, A, on the variations of the local Nusselt number, $Gr_x^{-1/4}Nu_x$, with the streamwise distance ξ for water vapour.

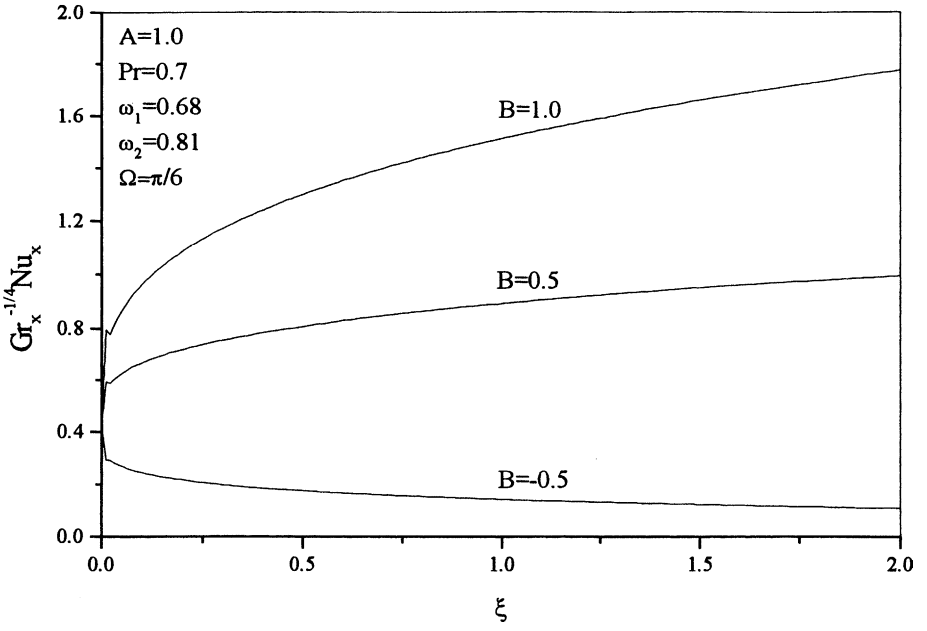

Fig. 14. Effect of the mass transfer parameter, B, on the variations of the local Nusselt number, $Gr_x^{-1/4}Nu_x$, with the streamwise distance ξ for air.

vapour for several values of A. Since the corresponding results for H_2, N_2 and CO are qualitatively similar to these results, for the sake of brevity, they are not shown here. Both the skin friction and the Nusselt number decrease with increasing streamwise distance ξ, because the momentum and thermal boundary layers grow with ξ. Also for a fixed ξ location, the skin friction coefficient and the Nusselt number decrease with increasing A. The reason for this behaviour is that the increase in A implies heating of the wall which in turn increases the viscosity of the gas. Consequently, both the momentum and thermal boundary layers increase which results in lower heat transfer and shear stress. Thus the variable gas properties exert a strong influence on the skin friction and heat transfer. In the case of water vapour, the trend of A on the heat transfer and skin friction is opposite to that of Ar, air and O_2. $A = 0$ implies that $T_w = T_\infty$ and the problem reduces to that with constant properties ($W_1 = W_2 = 1$, $W_3 = 0$, $N = N_1 = 1$). Since the results for $A = 0$ lie between $A = -0.25$ and $A = 0.25$, for the sake of clarity, they are not shown here.

The effect of the mass transfer parameter B on the local Nusselt number, $Gr_x^{-1/4}Nu_x$, for air is displayed in Fig. 14. Since the suction ($B > 0$) reduces the thermal boundary layer, the Nusselt number increases with suction, but decreases with increasing injection ($B < 0$).

5. Conclusions

The local skin friction and Nusselt number decrease with increasing wall temperature or streamwise distance. The variable gas properties significantly affect the heat transfer and skin friction. The effect of the wall temperature on the heat transfer and skin friction for water vapour

is found to be opposite to that of argon, air and oxygen. The heat transfer decreases with injection, but it increases with suction.

References

[1] B. Gebhart, Y. Jaluria, R.L. Mahajan, B. Sammakia, Buoyancy Induced Transport, Hemisphere, Washington, DC, 1988.
[2] E.M. Sparrow, J.L. Gregg, The variable fluid property problem in free convection, J. Heat Transfer 80 (1958) 871–886.
[3] A. Brown, The effect of laminar free convection heat transfer of temperature dependence of the coefficient of volumetric expansion, J. Heat Transfer 97 (1975) 133–135.
[4] D.D. Gray, A. Giogini, The validity of the Boussinesq approximation for liquids and gases, Int. J. Heat Mass Transfer 19 (1977) 545–551.
[5] M. Miyamoto, Influence of variable properties upon transient and steady-state free convection, Int. J. Heat Mass Transfer 20 (1977) 1258–1261.
[6] A.M. Clausing, S.N. Kempka, The influences of property variations on natural convection from vertical surfaces, J. Heat Transfer 103 (1981) 609–612.
[7] D.Y. Shang, B.X. Wang, Effect of variable thermophysical on laminar free convection of gas, Int. J. Heat Mass Transfer 33 (1990) 1387–1395.
[8] A. Pantokratoras, Laminar natural convection of pure and saline water along a vertical isothermal cylinder, Heat and Mass Transfer 36 (2000) 351–360.
[9] F.G. Blottner, Finite-difference method of solution of the boundary layer equations, AIAA J. 8 (1970) 193–205.
[10] T. Watanabe, Free convection boundary layer flow with uniform suction or injection over a cone, Acta Mech. 87 (1991) 1–9.
[11] A. Mucoglu, T.S. Chen, Mixed convection on inclined surfaces, J. Heat Transfer 101 (1979) 422–426.